stabilized per mole. This calculation leads to the values in the final column of Table V, -133 kcal/mol for $ZnCl_2$ and -25 kcal/mol for CuCl, a trend which agrees with the thermodynamic data. The agreement for $ZnCl_2$ is, of course, far from quantitative, which emphasizes that valence band energy stabilizations are only one important contribution to the total energy changes occurring upon covalent bonding.

Thus, Zn^{2+} complexes with σ-donor, π-donor ligands have large ionic and substantial covalent contributions to the chemical bonds. Both the ionic and covalent terms should be much smaller in the case of Cu^+. In particular, the low effective nuclear charge on Cu^+ together with the filled d levels and limited charge donation lead to weak bonding with donor ligands. The very low binding energy of the Cu^+ d^{10} levels, however, should make them readily accessible to back-bonding with π-acceptor ligands and lead to much stronger covalent interactions. In this regard, Cu^+ complexes with sulfur or CO ligands are, in fact, much more stable than the analogous Zn^{2+} complexes. Finally, we note that the low binding energies of Cu^+ d levels also lead to clear energy separation from the ligand levels, allowing the unobscured study of the d manifold, a fact which could have important implications in the PES study of the Cu(I)/Cu(II) redox couple.

Acknowledgment. We thank Dr. Andrew A. Gewirth for the SCF-Xα-SW calculation on $CuCl_4^{3-}$ and Professor T. Geballe for the gift of a CuCl sample. We acknowledge financial support of this research by the donors of the Petroleum Research Fund, administered by the American Chemical Society. The Stanford Synchrotron Radiation Laboratory, which is supported by the U.S. Department of Energy, has provided beam time, and the Stanford Center for Materials Research, supported by the Materials Research Division of the National Science Foundation, has provided experimental facilities for this research.

Registry No. ZnO, 1314-13-2; CuCl, 7758-89-6; $ZnCl_4^{2-}$, 15201-05-5.

Contribution from the Department of Chemistry, Texas A&M University, College Station, Texas 77843-3255

Electronic Structure of Metal Clusters. 6. Photoelectron Spectra and Molecular Orbital Calculations of Bis(μ_3-sulfido)- and Bis(μ_3-selenido)nonacarbonyltriosmium

Greg L. Griewe and Michael B. Hall*

Received June 22, 1987

Gas-phase, ultraviolet photoelectron (PE) spectra and molecular orbital (MO) calculations are reported for $Os_3(CO)_9(\mu_3\text{-}X)_2$ (X = S, Se). The spectra are similar to that reported for $Fe_3(CO)_9(\mu_3\text{-}S)_2$ but have increased band definition. The HOMO, a 3c-2e (Os-Os-Os) bond, is dominated by the e_g-like orbitals of the $Os(CO)_3$ fragment and contains most of the net metal-metal overlap population. Ionization from this orbital occurs at lower energy than the remaining ionizations. The t_{2g}-like orbitals on the $Os(CO)_3$ fragments make little or no net contribution to Os-X or to Os-Os bonding. The e_g-like and, to a lesser extent, the a_1-like orbitals on the metal fragments are responsible for nearly all of the Os-Os and Os-X (X = S, Se) bonds in the cluster.

Introduction

Metal clusters with bridging chalcogens are an important class of compounds. Chalcogens possess a wide range of possible coordination numbers and form relatively strong bonds to transition metals.[1] Triply bridging chalcogens contain a lone pair of electrons that can bond to unsaturated metal fragments[2] or to small clusters,[3] forming higher nuclearity clusters. They can also provide a convenient route to the preparation of mixed-metal clusters.[4] Several theoretical papers have appeared on $Fe_3(CO)_9(\mu_3\text{-}S)_2$,[5] which can be considered a model for more complicated systems. Rives et al.[5a] used Fenske-Hall molecular orbital calculations[6] to evaluate the bonding in an idealized model of $Fe_3(CO)_9S_2$ with 3-fold symmetry. They also used an empirical orbital localization procedure to determine which orbitals were bonds and which were lone pairs. Chesky et al.[5b] used Fenske-Hall calculations and He I photoelectron (PE) spectra to evaluate the bonding in $Fe_3(CO)_9S_2$ and related compounds with triply bridging sulfidos. The He II PE spectra have also been reported.[5c] The spectra in both papers consisted of two broad and relatively featureless groups of bands that were not amenable to detailed evaluation or comparison with the calculations.

This study will examine the bonding in $Os_3(CO)_9(\mu_3\text{-}X)_2$ (X = S, Se) using gas-phase, ultraviolet He I PE spectroscopy. The PE spectra will be interpreted by observing trends and comparing the spectra with parameter-free molecular orbital calculations. It is widely accepted that the spectra of second- and third-row homologues of first-row metal compounds have increased band definition due to spin-orbit coupling, kinematic effects of the heavier metal on the band envelope, and larger photoionization cross sections of 4d and 5d orbitals.[7] With enhanced definition of the PE spectra, comparison with the theoretical calculations should yield a more detailed understanding of the bonding in this class of clusters.

Experimental Section

$Os_3(CO)_9(\mu\text{-}S)_2$ and $Os_3(CO)_9(\mu_3\text{-}Se)_2$ were prepared according to a published procedure.[8] The ultraviolet photoelectron spectra were recorded on a Perkin-Elmer Model PS-18 spectrometer. The total spectra were recorded as single slow scans with the argon $^2P_{3/2}$ and $^2P_{1/2}$ lines at 15.76 and 15.94 eV, respectively, used as the internal reference. No free CO spike at 14 eV was observed, indicating that both compounds were stable and did not decompose in the spectrometer. The resolution for all spectra was better than 40 meV for the fwhm of the argon $^2P_{3/2}$ peak.

(1) (a) Adams, R. D.; Horvath, I. T.; Mathur, P.; Segmueller, B. E.; Yang, L. W. *Organometallics* **1983**, *2*, 1078. (b) Vahrenkamp, H. *Angew. Chem., Int. Ed. Engl.* **1975**, *14*, 322.

(2) (a) Adams, R. D. *Polyhedron* **1975**, *4*, 2003. (b) Adams, R. D.; Männing, D.; Segmueller, B. E. *Organometallics* **1983**, *2*, 149. (c) Winter, A.; Jibril, I.; Huttner, G. *J. Organomet. Chem.* **1983**, *242*, 259. (d) Seyferth, D.; Henderson, R. S.; Fackler, J. P., Jr.; Mazany, A. M. *J. Organomet. Chem.* **1981**, *213*, C21. (e) Richter, F.; Vahrenkamp, H. *Angew. Chem., Int. Ed. Engl.* **1978**, *17*, 444.

(3) (a) Adams, R. D.; Dawoodi, Z.; Foust, D. *Organometallics* **1982**, *1*, 411. (b) Adams, R. D.; Horvath, I. T.; Wang, L. W. *J. Am. Chem. Soc.* **1983**, *105*, 1533.

(4) (a) Adams, R. D.; Horvath, I. T.; Wang, S. *Inorg. Chem.* **1986**, *25*, 1617. (b) Adams, R. D.; Horvath, I. T.; Mathur, P. J. *J. Am. Chem. Soc.* **1983**, *105*, 7202. (c) Adams, R. D.; Horvath, I. T.; Segmueller, B. E.; Yang, L. W. *Organometallics* **1983**, *2*, 1301. (d) Adams, R. D.; Hor, T. S. A.; Horvath, I. T. *Inorg. Chem.* **1984**, *23*, 4733.

(5) (a) Rives, A. B.; Xiao-Zeng, Y.; Fenske, R. F. *Inorg. Chem.* **1982**, *21*, 2286. (b) Chesky, P. T.; Hall, M. B. *Inorg. Chem.* **1983**, *22*, 2998. (c) Van Dam, H.; Stufkens, D. J.; Oskam, A. *Inorg. Chim. Acta* **1978**, *31*, L377.

(6) Hall, M. B.; Fenske, R. F. *Inorg. Chem.* **1972**, *11*, 768.

(7) Higginson, B. K.; Lloyd, D. R.; Burroughs, P.; Gibson, D. M.; Orchard, A. F. *J. Chem. Soc., Faraday Trans. 2* **1973**, *69*, 1659.

(8) Johnson, B. F. G.; Lewis, J.; Raithby, P. R.; Hendrick, K.; McPartlin, M. *J. Chem. Soc., Chem. Commun.* **1979**, *16*, 719.

0020-1669/88/1327-2250$01.50/0

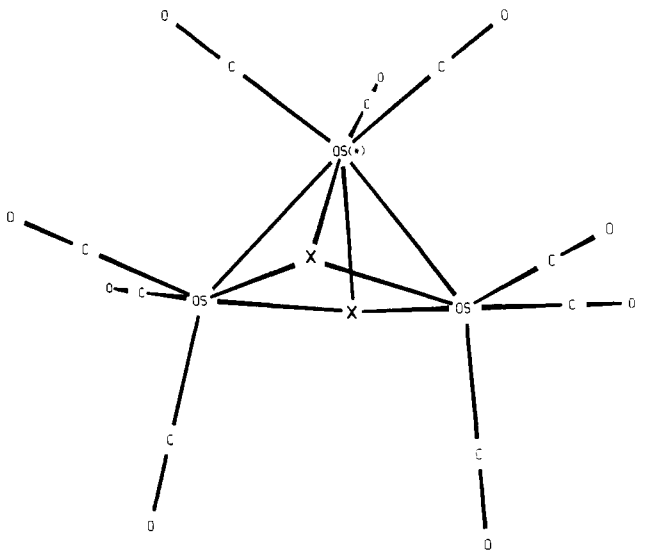

Figure 1. Structure and coordinate system for $Os_3(CO)_9(\mu_3\text{-}X)_2$ (X = S, Se). The *xy* plane contains the three Os atoms, and the *yz* plane contains the unique metal (Os*), one of its carbonyls, and the bridging chalcogens.

Fenske–Hall molecular orbital calculations[6] were performed on the Department of Chemistry's VAX 11/780 computer. Since suitable basis functions are unavailable for Os, the actual calculations were done for $Ru_3(CO)_9(\mu_3\text{-}X)_2$ (X = S, Se) but will be referred to as if they were done on the Os clusters. The Ru basis functions were taken from Richardson et al.[9] and were augmented by 5s and 5p functions with exponents of 2.20. The carbon, oxygen, sulfur, and selenium functions were taken from the double-ζ functions of Clementi[10] and reduced to single-ζ functions,[11] except for the p valence functions, which were retained as the double-ζ function. The atomic functions were made orthogonal by the Schmidt procedure. Mulliken population analysis[12] was used to determine both the individual atomic charges and the atomic orbital populations.

Since the covalent radii of Ru and Os are very similar,[13] the atomic positions for the calculations were taken from the crystal structures of $Os_3(CO)_9(\mu_3\text{-}X)_2$ (X = S,[14] Se[15]). The geometries were optimized only slightly to C_s. The mirror plane (*yz* plane in Figure 1) contains the unique metal, one of its carbonyls, and the bridging chalcogen atoms. The Os–C and C–O bond lengths were held fixed in both clusters. The Os–Os and Os–X (X = S, Se) distances are slightly larger in the Se homologue, presumably, because of the larger covalent radius of Se.[13]

Koopmans' theorem[16] states that each IE can be associated with the negative of the molecular orbital energy. In spite of its well-documented quantitative failures,[17] it is convenient to describe ionizations in terms of the molecular orbitals in the ground-state neutral molecule. Thus, the application of Koopmans' theorem is an adequate approximation if the errors it introduces (which are due to relaxation and spin-orbit effects) are relatively constant. Large relaxation effects are often due to ionizations from localized orbitals.[18] The metal–metal interactions for third-row transition metals are strong, and the 5d orbitals are relatively diffuse. Therefore, Os valence electrons are less likely to localize upon ionization. The net result is that Koopmans' theorem should be more accurate for a third-row metal complex.[19] Even if it is not exact, it forms a useful approximation as long as the reader understands that our description of the character of ionic states is approximate.

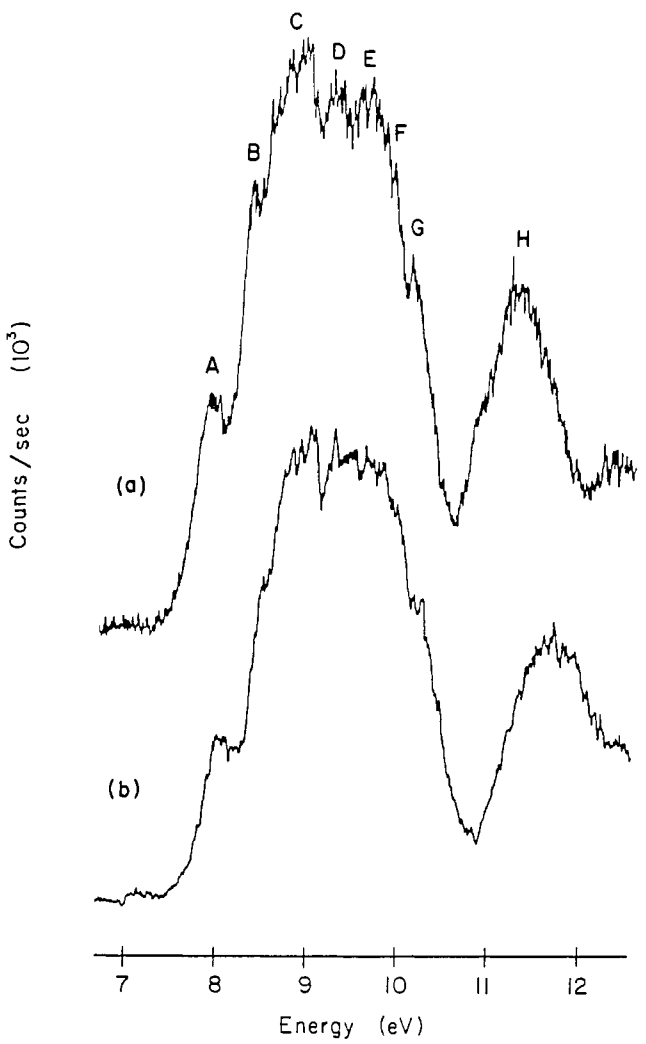

Figure 2. Partial photoelectron spectra of (a) $Os_3(CO)_9Se_2$ and (b) $Os_3(CO)_9S_2$.

Table I. Absolute Values for Ionization Energy Peak Maxima (eV) in $Os_3(CO)_9(\mu_3\text{-}X)_2$ (X = S, Se)

	sulfido		selenido	
band	IP	assgnt	IP	assgnt
A	8.02	7a″	7.92	7a″
B	8.50	9a′	8.30	9a′
C	8.90	6a″–8a′	8.76	6a′–8a′
D	9.32	5a′, 6a′	9.17	5a′
E	9.65	4a″, 5a″	9.51	4a″, 5a″
F	9.89	4a′	9.81	4a′
G	10.15	3a″	10.04	3a″
H	11.56	1a′–3a′	11.18	1a′–3a′

The complete analysis of the spectra of molecules containing third-row transition metals should take into account spin–orbit coupling. Detailed spin–orbit coupling treatments have been used to interpret the PE spectra of mononuclear third-row transition-metal complexes.[20] However, a detailed spin–orbit analysis of these triosmium clusters is not justified by the spectral resolution. Therefore, we used only qualitative spin–orbit arguments to describe the primarily metal ionizations in the spectra.

Results

Photoelectron Spectra. The ionization energy (IE) range of interest spans 7–13 eV. The IE region above 13 eV will not be discussed because of the normally broad and poorly resolved bands due to the carbonyl 5σ and 1π ionizations. The partial photoelectron spectra are shown in Figure 2. These spectra are characterized by a broad set of bands (7.5–10.5 eV) with two

(9) Richardson, J. W.; Blackman, M. J.; Ranochak, J. E. *J. Chem. Phys.* **1973**, *58*, 3010.
(10) (a) Clementi, E. J. *J. Chem. Phys.* **1964**, *40*, 1944. (b) Clementi, E. J. *IBM J. Res. Dev.* **1965**, *9*, 2.
(11) Fenske, R. F.; Radtke, D. D. *Inorg. Chem.* **1968**, *7*, 479.
(12) Mulliken, R. S. *J. Chem. Phys.* **1955**, *23*, 1833, 1841.
(13) Moeller, T. *Inorganic Chemistry, A Modern Introduction*; Wiley: New York, 1982; p 70.
(14) Adams, R. D.; Horvath, I. T.; Segmueller, B. E.; Yang, L. W. *Organometallics* **1983**, *2*, 144.
(15) Johnson, B. F. G.; Lewis, J.; Lodge, P. G.; Raithby, P. R. *Acta Crystallogr., Sect. B: Struct. Crystallogr. Cryst. Chem.* **1981**, *B37*, 1731.
(16) Koopmans, T. *Physica (Amsterdam)*, **1934**, *1*, 104.
(17) (a) Evans, S.; Guest, M. F.; Hillier, I. H.; Orchard, A. F. *J. Chem. Soc., Faraday Trans 2* **1974**, *70*, 417. (b) Coutiere, M.; Demuynck, J.; Veillard, A. *Theor. Chim. Acta*, **1972**, *27*, 281.
(18) Calabro, D. C.; Lichtenberger, D. L. *Inorg. Chem.* **1980**, *19*, 1732.
(19) Chesky, P. T.; Hall, M. B. *Inorg. Chem.* **1983**, *22*, 2104.
(20) (a) Hall, M. B. *J. Am. Chem. Soc.* **1975**, *97*, 2057. (b) Lichtenberger, D. L.; Fenske, R. F. *J. Am. Chem. Soc.* **1976**, *98*, 50.

Table II. Atomic Composition of $Os(CO)_3$ Fragments

	% atomic compn				
orbital	Os 5d	Os 6s	Os 6p	CO 5σ	CO 2π
a_1	13	19	33		36
e_g	42		29	6	22
t_{2g}	75				22

distinct shoulders on the low-energy side (bands A and B) and two shoulders on the high-energy side (bands F and G). A small energy gap separates the broad set of bands from a weaker and narrower band (band H). The ionization energies and assignments of the bands are given in Table I.

Molecular Orbital Calculations. In large molecules such as trinuclear clusters, the complexity of the MO pattern becomes difficult to interpret because of the closely spaced molecular orbitals. This problem is simplified by fragment analysis, where one views these clusters as formed from three $Os(CO)_3$ fragments and two bridging chalcogens. This approach has been successfully applied to describe the bonding in trimetallic nonacarbonyl clusters.[21]

The lowest lying valence molecular orbitals of the osmium carbonyl fragments consist of symmetry-adapted combinations of the carbonyl 3σ, 4σ, and 1π orbitals and the Os–CO σ bonds formed by donation from the carbonyl 5σ orbitals to the metal orbitals. These 15 low-lying orbitals on each fragment do not contribute to cluster bonding and will not be discussed further.

The metal orbitals of the $Os(CO)_3$ fragments can be classified as t_{2g}-, e_g-, or a_1-like.[22] The lowest of these, the t_{2g}-like orbitals, are at a much higher energy than the Os–CO σ-bonding orbitals and are predominantly Os d in character. The t_{2g}-like set, which has d orbitals with lobes between the Os–C internuclear axes, is stabilized by Os $d\pi$ to CO 2π back-donation. The next two orbitals correspond to the e_g orbitals of an octahedral system. The e_g-like set, which has d orbitals with lobes along the Os–C internuclear axis, is destabilized by CO 5σ to Os $d\sigma$ donation. The e_g-like orbitals also contain a significant amount of Os p character. Further destabilized is the a_1-like orbital. The a_1-like fragment orbital contains more Os s and p character than d character, as well as more CO 2π character than the e_g-like orbitals. The atomic characters of the most important fragment orbitals for the cluster formation are listed in Table II.

All three $Os(CO)_3$ fragments have C_s symmetry. In spite of this low symmetry, the energy gaps between the t_{2g}-like orbitals are small (~0.1 eV) and the energy gap between the e_g-like orbitals is also relatively small (~0.3 eV). In the neutral fragment, the lower energy e_g-like orbital is the HOMO and the other is the LUMO. The small energy gaps among the t_{2g}- and e_g-like orbitals contrast with the large t_{2g}–e_g splitting (5.2 eV). This result is consistent with the large crystal field splitting expected for a second- or third-row transition metal ligated by carbonyls.[23] The t_{2g}-e_g splitting calculated for $Fe(CO)_3$ fragments in $Fe_3(CO)_9S_2$ was only 2.9 eV.[5b]

The bridging chalcogens are far enough apart (d_{S-S} = 3.07 Å, d_{Se-Se} = 3.25 Å) that they do not interact with one another. Only their p orbitals are available for cluster bonding, because the s orbitals in S and the s and d orbitals in Se are far too stable to interact to any significant extent with the $Os(CO)_3$ fragments.

The $Os_3(CO)_9(\mu_3\text{-}X)_2$ cluster formation will be described in terms of the higher energy orbitals of the three $Os(CO)_3$ fragments and the p orbitals of the bridging chalcogens. The MO bonding scheme for the formation of the clusters from the fragments is shown in Figure 3.

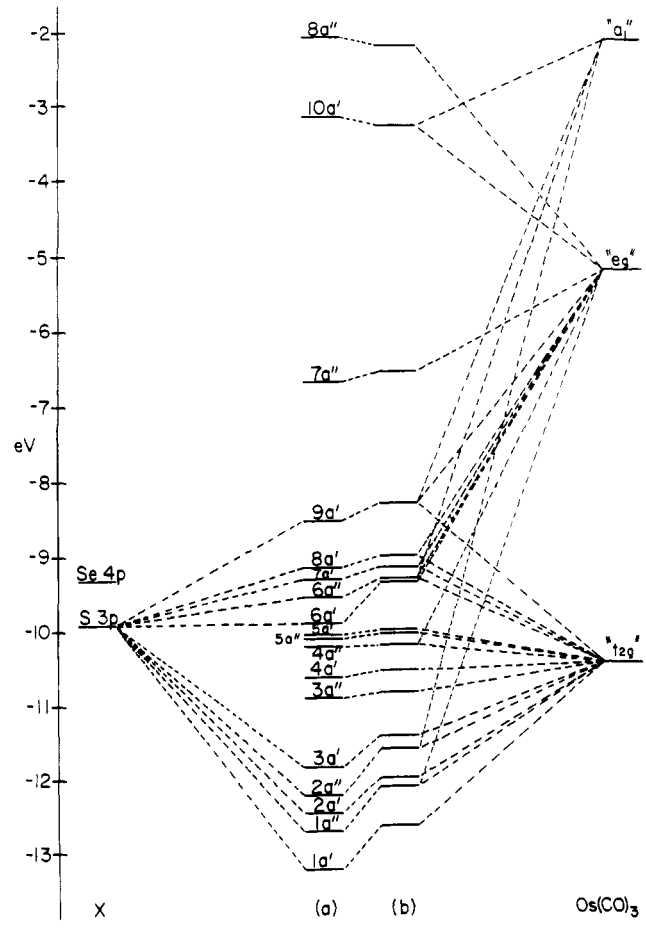

Figure 3. Molecular orbital diagrams for (a) $Os_3(CO)_9S_2$ and (b) $Os_3(CO)_9Se_2$. The energy values were obtained from Fenske–Hall calculations. 7a'' is the HOMO.

The HOMO (7a''), the LUMO (10a'), and the second lowest unoccupied molecular orbital (8a'') are all derived from the same three e_g-like fragment orbitals. 7a'' is the in-phase combination and is metal–metal bonding. 10a' is metal–metal nonbonding, and 8a'' is strongly metal–metal antibonding. As shown in Table III, 10a' and 8a'' contain some chalcogen character while 7a'' contains none. Both 10a' and 8a'' are strongly metal–chalcogen antibonding. It is clear from the calculations that the large HOMO–LUMO gap is not due to metal–metal interactions but to metal–chalcogen interactions.

The HOMO in the clusters, represents a three-center, two-electron (3c-2e) Os–Os–Os bond and contains 79% of the net metal–metal bonding character, as shown in Table IV. There is also some metal–metal bonding character in the second highest occupied molecular orbital (9a') as well as in more stabilized orbitals (1a'–3a''). However, nearly all of the metal–metal bonding in the 1a'–3a'' orbitals is cancelled by the 5a'–8a' orbitals, which are somewhat metal–metal antibonding.

Orbitals 1a'–3a'' are primarily responsible for Os–X bonding with orbitals 4a'', 6a'', 7a', 9a', and especially 6a' also contributing to the metal–chalcogen bonds. Reduced symmetry allows mixing of the t_{2g}-, e_g-, and a_1-like orbitals on the metal fragments, adding some confusion to the bonding picture. Although, as shown in Table IV, the fragment t_{2g}-like orbitals contribute significantly to metal–chalcogen bonding in the lower five orbitals (1a'–3a''), this bonding interaction is cancelled by antibonding interactions in the upper orbitals since all molecular orbitals derived from the t_{2g}-like orbitals are filled. As shown in Table V, nearly all of the net Os–Os and Os–X bonding is through the e_g- and a_1-like orbitals.

Discussion

Spectra and Calculations. The calculated one-electron energies obtained from the Fenske–Hall calculations correlate reasonably

(21) (a) Chesky, P. T.; Hall, M. B. *Inorg. Chem.* **1981**, *20*, 4419. (b) Sherwood, D. E., Jr.; Hall, M. B. *Organometallics* **1982**, *1*, 1519. (c) Chesky, P. T.; Hall, M. B. *Inorg. Chem.* **1983**, *22*, 3327.
(22) (a) Elian, M.; Hoffman, R. *Inorg. Chem.* **1975**, *14*, 1058. (b) Hoffmann, R. *Science (Washington, D.C.)* **1981**, *211*, 995. (c) Hoffmann, R. *Angew. Chem., Int. Ed. Engl.* **1982**, *21*, 711.
(23) (a) Figgis, B. N. *Introduction to Ligand Fields*; Wiley-Interscience: New York, 1966. (b) Cotton, F. A.; Wilkinson, G. *Advanced Inorganic Chemistry*, 4th ed.; Wiley-Interscience: New York, 1980.

Table III. Molecular Composition of $Os_3(CO)_9(\mu_3\text{-}X)_2$ (X = S, Se)

	% fragment compn							
	t_{2g}		e_g		a_1		X	
orbital	S	Se	S	Se	S	Se	S	Se
8a″	2	2	87	86	1	2	5	8
10a′	6	6	74	72	5	6	14	15
7a″	3	3	94	94	2	3		
9a′	47	41	14	16	11	12	27	31
8a′	57	49	9	13	2	1	31	36
7a′	58	46	13	13	1	3	28	38
6a″	60	49	9	12	8	10	21	28
6a′	16	13	18	21			64	64
5a′	89	93	2	1	1	1	7	4
5a″	96	92		1	2	3	1	4
4a″	77	76	11	11	1		11	13
4a′	94	94	1	1			4	4
3a″	93	92	3	3			3	4
3a′	38	52	8	5	4	3	49	39
2a″	32	40	8	10	8	6	49	43
2a′	44	51	5	5	1	1	49	43
1a″	33	42	16	14	2	2	48	38
1a′	42	51			3	4	55	50

Table IV. Mulliken Overlap Populations of $Os_3(CO)_9Se_2$ by Molecular Orbital

	overlap populations										
	Os*–Os[a]							Os–Se[b]			
orbital	t_{2g}–t_{2g}	t_{2g}–e_g	t_{2g}–a_1	e_g–e_g	e_g–a_1	a_1–a_1	tot.	t_{2g}–Se	e_g–Se	a_1–Se	tot.
7a″		−0.006	−0.001	0.069	0.019		0.081				
9a′	0.003	0.004	−0.006	0.003	0.005	0.010	0.016	−0.105	0.062	0.103	0.060
8a′		−0.007	−0.003	0.002	0.001	−0.001	−0.008	−0.095	0.083	0.017	0.005
7a′	0.004	−0.007	−0.001	0.003	0.001	0.002	0.002	−0.095	0.079	0.052	0.037
6a″	0.001	0.003	−0.009	−0.005	0.006		−0.004	−0.098	0.051	0.094	0.047
6a′		−0.003		−0.006			−0.009	−0.012	0.127		0.115
5a′	−0.014	0.003	0.003		0.001	−0.001	−0.008	−0.003	0.008	0.003	0.008
5a″	−0.013		0.007		−0.002		−0.008	−0.005	0.003	0.015	0.013
4a″								−0.022	0.074	0.002	0.054
4a′	−0.002	0.001	0.001					0.010	0.001	0.001	0.012
3a″	0.005	0.002		0.001			0.008	0.009	0.008		0.017
3a′	−0.001	0.003	0.005		0.001		0.009	0.077	0.047	0.029	0.153
2a″			0.001	−0.001	0.003		0.003	0.055	0.082	0.051	0.188
2a′	0.003	0.003	0.001			−0.001	0.006	0.102	0.047	0.028	0.177
1a″	0.005	0.003	0.003		0.001		0.012	0.062	0.122	0.020	0.204
1a′	0.007	0.001	0.004			0.001	0.013	0.101	0.004	0.044	0.149

[a] Overlap populations between the unique osmium, Os*, and one of the other osmiums. [b] Overlap populations between the seleniums and all three osmiums.

Table V. Mulliken Overlap Populations for $Os_3(CO)_9X_2$ (X = S, Se)

	overlap populations[a]									
	t_{2g}–t_{2g}	t_{2g}–e_g	t_{2g}–a_1	e_g–e_g	e_g–a_1	a_1–a_1	t_{2g}–X	e_g–X	a_1–X	tot.
					$Os_3(CO)_9S_2$					
Os*–Os	−0.003	−0.001	0.003	0.070	0.030	0.004				0.103
Os–Os		−0.003	−0.007	−0.010		−0.009				−0.030
Os*–S							0.001	0.112	0.078	0.191
Os–S							−0.006	0.146	0.081	0.221
					$Os_3(CO)_9Se_2$					
Os*–Os	−0.002	−0.001	0.003	0.066	0.033	0.005				0.104
Os–Os		−0.003	−0.004	−0.007		−0.008				−0.024
Os*–Se							0.002	0.116	0.080	0.198
Os–Se							−0.005	0.152	0.079	0.226

[a] Os* is the unique osmium in every case.

well with the observed ionization energies in the PE spectra,[24] but because these calculations are approximate, there are some significant differences, especially for molecular orbitals of vastly different compositions. The most profound example of this is the gap between bands A and B, which is exaggerated in the calculations. As shown in Table III, band A is composed entirely of e_g-like orbitals, in contrast to band B, which has only a small amount of e_g-like character. Most of the other gaps match the spectra fairly well.

Every band shown for $Os_3(CO)_9S_2$ shifts to a lower energy in the Se homologue. This is also reflected in the calculations. The biggest shifts are seen in bands containing the largest amounts of chalcogen character (i.e. 1a′–3a″ in band H, which shifts by ~0.4 eV). These shifts are readily explained because the ionization energy of Se 4p orbitals is lower than that of S 3p orbitals.

(24) (a) Lichtenberger, D. L.; Fenske, R. F. *Inorg. Chem.* **1976**, *15*, 2015. (b) Block, T. F.; Fenske, R. F. *J. Am. Chem. Soc.* **1977**, *99*, 4321. (c) Hubbard, J. L.; Lichtenberger, D. L. *Inorg. Chem.* **1980**, *19*, 1388. (d) Morris-Sherwood, B. J.; Kolthammer, B. W. S.; Hall, M. B. *Inorg. Chem.* **1981**, *20*, 2771. (e) DeKock, R. L.; Wong, K. S.; Fehlner, T. P. *Inorg. Chem.* **1982**, *21*, 3203.

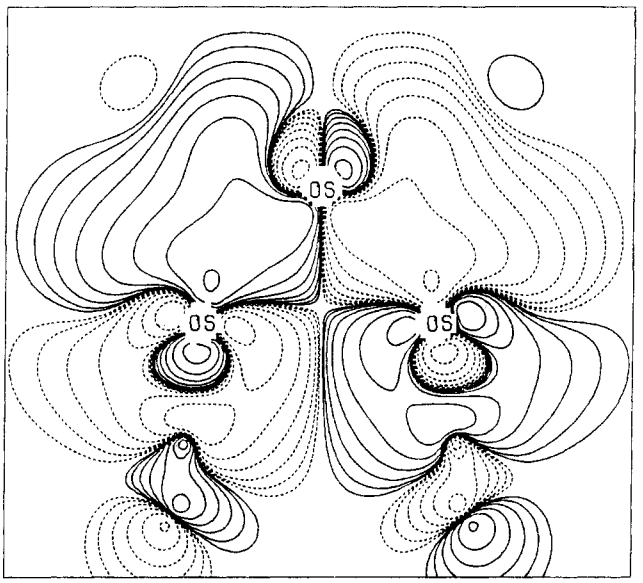

Figure 4. Orbital plot of 7a″ in the *xy* plane of $Os_3(CO)_9Se_2$. The lowest contour values are 2.44×10^{-4} e au^{-3}, and each succeeding contour differs from the previous one by a factor of 2.0.

One of the remaining largest shifts in the calculations is that of 6a′. The calculations suggest that orbital 6a′ shifts from band D in $Os_3(CO)_9S_2$ to band C in the Se homologue. This shift can be seen in the spectra, with band D narrower and the high-energy side of band C more intense in the Se homologue than the corresponding bands in the S homologue.

Nearly all of the band assignments can easily be made from the calculations, except for bands D and E. In order to interpret bands D and E, spin–orbit coupling effects must be taken into consideration. Certainly, with the exception of 6a′ in $Os_3(CO)_9S_2$, bands D and E are composed almost entirely of t_{2g}-like fragment orbitals. The calculated energies of orbitals 5a′ and 5a″ are very close. Since orbitals 5a′ and 5a″ have very large characters on the same metal (both have 43% t_{2g}-like character on the unique osmium) and are very close in energy, it is reasonable to infer that these two orbitals would be strongly split by spin–orbit coupling, with 5a′ destabilized to form band D and 5a″ stabilized, joining 4a″ to form band E. Although the assignments of bands D and E are less certain than those of the other bands, they are reasonable deductions based on the available information.

The assignments given in Table I depend heavily on the correlations with the molecular orbital calculations, especially for the closely spaced bands C–F, and must be viewed with some caution. Although Fenske–Hall calculations are often better than other methods in making these assignments, and the assignments of bands C–F fit nicely with the qualitative change in the intensity of bands C and D and with the most important spin–orbit effects in bands D and E, our assignments for this central region remain tentative.

He I and He II PE spectra for the isostructural compound $Fe_3(CO)_9S_2$ have already appeared.[5b,c] The $Os_3(CO)_9X_2$ (X = S, Se) He I spectra show the same general features as the $Fe_3(CO)_9S_2$ spectrum. The differences are that in the Os homologue spectra the first group of bands (A–G) are better resolved than in those of the Fe homologue, and they are much more intense (relative to band H) in the Os spectra. These differences are due to spin–orbit coupling and to the "heavy-atom effect".[7] Previous extended Hückel[5c] and Fenske–Hall[5b] calculations have attributed the breadth of the first group of bands in $Fe_3(CO)_9S_2$ to the presence of two different kinds of Fe atoms. In contrast, the osmium homologues have similarly charged metal atoms (e.g. in $Os_3(CO)_9Se_2$, the charge on Os* (Os* is the unique Os) is +0.189 and the charge on Os is +0.227). The smaller charge difference and the larger metal–metal overlap in these heavier congeners result in more mixing of the different Os atoms in the molecular orbitals. Thus, for these osmium homologues we would not assign the high-energy side of the first group of bands to Os* nor the low-energy side to the nonunique osmiums, as was done for the irons in the Fe homologue.

In the series $SH_2M_3(CO)_9$ (M = Fe, Ru, Os), the PE spectra[5b] show trends similar to those described above. Our explanation for the trends is similar except for the emphasis on the charge separation in $Fe_3(CO)_9S_2$. In comparing the PE spectra of $Fe_3(CO)_9S_2$ and $SH_2Fe_3(CO)_9$,[5b] one observes a somewhat wider metal band for $Fe_3(CO)_9S_2$, which we attribute to an increase in the charge separation of the three iron atoms in $Fe_3(CO)_9S_2$ relative to that in $SH_2Fe_3(CO)_9$.

Nature of the Bonding. According to skeletal electron pair theory[25] (SEP), each $Os(CO)_3$ fragment donates two electrons and each X donates four electrons for a total of seven pairs of electrons available for cluster bonding. Thus, these molecules are nido clusters, based on a six-vertex polyhedron with one vertex missing and seven electron pairs in seven bonding orbitals. The crystal structures show a bond between each osmium and the bridging ligands and between the unique osmium and the other two osmiums for a total of eight bonds. Clearly, with eight bonded edges and seven electron pairs, a 3c-2e bond is required in a simple valence description of the bonding. The calculations suggest that structures **1** and **2** are important resonance structures. The

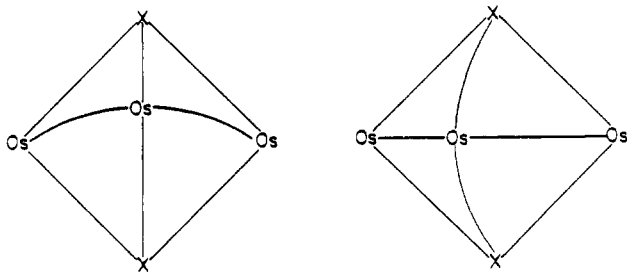

1 **2**

HOMO in our clusters, 7a″, contains most of the Os*–Os (Os* is the unique Os) overlap population and looks very much like a 3c-2e bond (as shown in Figure 4). The "expected" overlap population between two osmium atoms in a 3c-2e bond, based on the overlap population of 0.131 for a single 2c-2e bond in $(\mu\text{-}H)_2Os_3(CO)_{10}$,[26] is 0.066. The Os*–Os overlap population in $Os_3(CO)_9S_2$ is 0.103, roughly halfway between a 3c-2e and a 2c-2e bond. The overlap population between Os* and a bridging S is 0.191, fairly close to 0.221, the overlap population between Os and S. The smaller overlap population between Os* and S is a reflection of its slightly longer bond length (d_{Os^*-S} = 2.444 Å, d_{Os-S} = 2.400 Å). The Os*–Os bond is not as long as would be expected if a 3c-2e bond were the sole Os*–Os interaction. The Os*–Os bond length of 2.813 Å in $Os_3(CO)_9S_2$ is shorter than an Os–Os bond in $Os_3(CO)_{12}$[27] (d_{Os-Os} = 2.877 Å) and nearly the same as the Os*–Os single bond in $H_2Os_3(CO)_{10}$[28] (d_{Os^*-Os} = 2.815 Å). Thus, the calculated overlap populations suggest that **1** is somewhat more important than **2**. The reported Os–Os and Os–S bond lengths would suggest that neither of these resonance structures is adequate and that SEP theory is unable to explain the bonding in these clusters. Since both the Os–S and Os–Os bonds appear to be full single bonds, an additional electron pair is required for an all-single-bonded structure. This pair could be supplied by one of the t_{2g}-like fragment orbitals.

Adams has demonstrated the synthetic utility of $Os_3(CO)_9S_2$ in the preparation of higher nuclearity clusters.[2a,b] It is believed that the lone pairs of electrons on the bridging sulfidos serve as the initial point of attack for an incoming electrophilic metal group.[1-4]

Orbital 6a′ in $Os_3(CO)_9S_2$ is the highest occupied orbital that contains a substantial amount (64%) of S character. An orbital plot of 6a′ is shown in Figure 5. Although orbital 6a′ contains some osmium–sulfur bonding character, it is relatively localized

(25) Wade, K. *Adv. Inorg. Chem. Radiochem.* **1976**, *18*, 1.
(26) Sherwood, D. E., Jr.; Hall, M. B. *Inorg. Chem.* **1982**, *21*, 3458.
(27) Churchill, M. R.; DeBoer, B. G. *Inorg. Chem.* **1977**, *16*, 878.
(28) Broach, R. W.; Williams, J. M. *Inorg. Chem.* **1979**, *18*, 314.

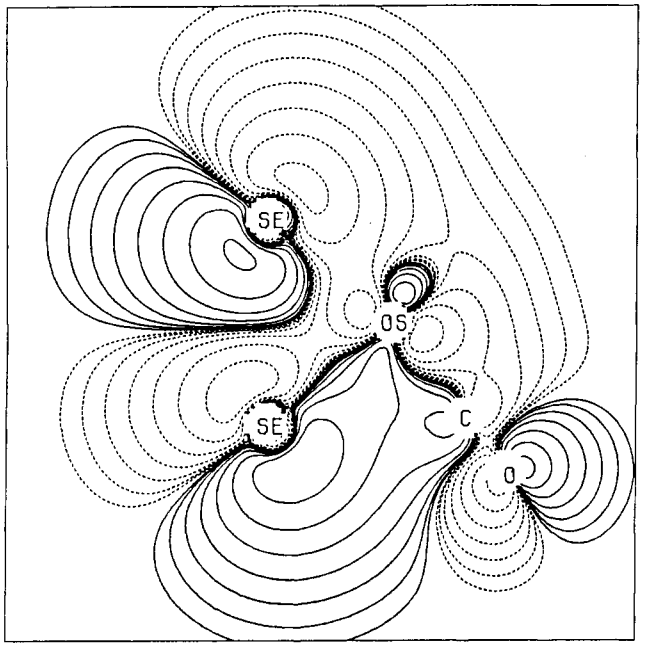

Figure 5. Orbital plot of 6a′ in the *yz* (mirror) plane. The lowest contour values are 2.44×10^{-4} e au^{-3}, and each succeeding contour differs from the previous one by a factor of 2.0.

on S and has substantial lone-pair character. We believe that 6a′ plays an important role in these condensation reactions. For example, in the insertion of a PtL_2 fragment into an Os*–S bond, the crystal structure of the insertion product[4d] shows the PtL_2 fragment opposite the unique carbonyl on Os* (Pt–Os*–C ≃ 166°). This stereochemistry would be consistent with electrophilic attack on the Os*–S bond opposite the unique carbonyl. Our calculations show that the amount of S character in the 6a′ orbital is twice as large for the S opposite the unique carbonyl (the upper chalcogen in Figure 5) as it is for the other S (43% vs 21%). Thus, the upper S has the more available chalcogen electrons. This is also reflected in the relative numbers of contours in Figure 5.

To date, only $Os(CO)_4$ has been inserted into an osmium–chalcogen bond in $Os_3(CO)_9Se_2$.[29] Because of very similar electronic structures and with even more available chalcogen electron density (6a′ is destabilized by 0.56 eV) than in the S homologue, $Os_3(CO)_9Se_2$ should develop a condensation chemistry comparable to that of $Os_3(CO)_9S_2$.

(29) Adams, R. D.; Horvath, I. T. *Inorg. Chem.* **1984**, *23*, 4718.

Conclusion

Through the study of Os homologues of $Fe_3(CO)_9S_2$ we have clarified the bonding and spectral assignments of these clusters. The HOMO is a M–M–M 3c-2e bond that contains most of the metal–metal bonding population. Nearly all of the net cluster bonding uses the e_g- and a_1-like fragment orbitals. The t_{2g}-like fragment orbitals mix heavily into the cluster bonding and antibonding orbitals but result in little net contribution to metal–metal or metal–chalcogen bonds. The metal–chalcogen interactions are much stronger than the metal–metal interactions, as demonstrated in the relative gaps between orbitals 7a″, 10a′, and 8a″.

In $Fe_3(CO)_9S_2$ all of the orbitals with substantial sulfur character were beneath the molecular orbitals derived solely from the t_{2g}-like sets. In the osmium homologues there was an orbital (6a′) with substantial chalcogen character in the midst of the t_{2g}-derived orbitals. The calculations show that 6a′ is destabilized by 0.56 eV when S is replaced by Se. This shift from band D to band C can be seen in the spectra of $Os_3(CO)_9X_2$, X = S and Se, respectively. We believe that 6a′ has substantial chalcogen lone-pair character, which we propose is important in the nucleophilic attack of this cluster on metal–ligand groups containing low-lying unoccupied orbitals.

We are unable to reconcile resonance structures **1** and **2** with the observed structures of the osmium clusters. All metal–metal and metal–chalcogen bonds appear to be full single bonds. A possible solution of this dilemma would be the addition of an electron pair beyond the seven pairs required by SEP theory. A potential source of this extra electron pair may be one of the fragment t_{2g}-like orbitals. The only alternative would be to assume that the Os–Os bond lengths are insensitive to the Os–Os bond order and that the calculations, which favor resonance structure **1**, are essentially correct.

Acknowledgment. We thank the Robert A. Welch Foundation (Grant No. A-648) for the support of this work and the National Science Foundation for funds to purchase the VAX 11/780.

Registry No. $Os_3(CO)_9(\mu_3\text{-}S)_2$, 72282-40-7; $Os_3(CO)_9(\mu_3\text{-}Se)_2$, 72282-41-8.

Contribution from the Department of Chemistry, Colorado State University, Fort Collins, Colorado 80523, and Los Alamos National Laboratory, Los Alamos, New Mexico 87545

Electronic and Molecular Structure of $OTeF_5^-$

P. K. Miller,[1a] K. D. Abney,[1b] A. K. Rappé,[1a] O. P. Anderson,[1a] and S. H. Strauss*,[1a,2]

Received November 3, 1987

Salts of the $OTeF_5^-$ anion were investigated by IR and Raman spectroscopy and by X-ray crystallography. Experimental results were compared with ab initio Hartree–Fock calculations on the $OTeF_5$ radical, $Na^+OTeF_5^-$, and the singlet and triplet states of the free $OTeF_5^-$ anion. The compound $[(PS)H^+][OTeF_5^-]$ was examined by single-crystal X-ray crystallography ($(PS)H^+$ = protonated 1,8-bis(dimethylamino)naphthalene): $P\bar{1}$, a = 8.241 (1) Å, b = 8.768 (2) Å, c = 12.591 (3) Å, α = 74.08 (2)°, β = 78.00 (2)°, γ = 80.23 (2)°, Z = 2, T = −106 °C. Unlike other salts of the $OTeF_5^-$ anion, $[(PS)H^+][OTeF_5^-]$ did not exhibit any O/F disorder. Since the spectroscopic data for $[(PS)H^+][OTeF_5^-]$ closely matched those of $[N(n\text{-}Bu)_4^+][OTeF_5^-]$, it was concluded that this structure contains the best approximation of the structure of the free $OTeF_5^-$ anion. The librationally corrected results are Te–O = 1.803 Å, Te–F_{ax} = 1.872 Å, Te–F_{eq} = 1.870 Å (average), and O–Te–F_{eq} = 95.2° (average). A normal-coordinate analysis of $OTeF_5^-$ was carried out by using this geometry and spectroscopic data for the ^{16}O and ^{18}O equivalents of $[N(n\text{-}Bu)_4^+][OTeF_5^-]$.

Introduction

Studies of metal and non-metal $OTeF_5$ (teflate) compounds have been aided by the spectroscopic and structural probes afforded by the $OTeF_5$ group: the Te–O distance, the TeO stretching frequency (ν(TeO)), and the ^{19}F NMR chemical shift of the fluorine atom trans to oxygen.[3-8] These parameters vary

(1) (a) Colorado State University. (b) Los Alamos National Laboratory.
(2) Alfred P. Sloan Fellow, 1987–1989.

(3) Strauss, S. H.; Abney, K. D.; Anderson, O. P. *Inorg. Chem.* **1986**, *25*, 2806.

0020-1669/88/1327-2255$01.50/0